Predicting the Equilibrium Product Formation in Oxy-fuel Combustion of Octane (C_8H_{18}) using Numerical Modeling

Fabiano Fernandes Bargos
Department of Basic and Environmental Sciences, Lorena School of Engineering, University of Sao Paulo, Brazil
fabianobargos@usp.br

Estaner Claro Romao
Department of Basic and Environmental Sciences, Lorena School of Engineering, University of Sao Paulo, Brazil
estaner23@usp.br (corresponding author)

Received: 24 March 2023 | Revised: 12 April 2023 | Accepted: 14 April 2023

 DOI: https://doi.org/10.48084/etasr.5881

ABSTRACT

Preserving the environment is a major challenge for modern society, and reducing the greenhouse effect caused by combustion processes is a primary concern. It is known that nitrogen compounds (NO_x) negatively impact air quality and public health. Internal combustion engines, responsible for nearly half of the atmosphere's pollutants, have prompted public policymakers to phase out gasoline and diesel-powered vehicles in the near future. Carbon capture and storage technologies, including oxy-fuel combustion, are being developed to address these environmental challenges. To predict exhaust pollutants such as NO and CO, assuming that the exhaust gases resulting from fuel and air combustion are in chemical equilibrium is a useful approximation. In the current case study, a numerical investigation on the impact of modifying the oxygen content of the reaction mixture from 21% to 100% on the equilibrium composition of C_8H_{18} air-enriched combustion was conducted. Specifically, the equilibrium-constant approach routines were tailored for 10 species reported in the literature to the conditions of oxy-fuel combustion. Additionally, a comprehensive analysis was performed by varying the temperature and equivalence ratio alongside the oxygen level. The results emphasize the intricate interplay between various factors in oxy-combustion and provide valuable insight into the equilibrium product formation in oxy-fuel combustion. Notably, the non-uniform reduction of N_2 as a function of O_2 is highlighted, with an overall reduction rate of 0.93 observed across the range of O_2 percentages from 21% to 99%.

Keywords- air pollution; carbon capture and storage; nitrogen compounds; air-enriched combustion

I. INTRODUCTION

The reduction of greenhouse gas emissions, particularly carbon dioxide (CO_2) from combustion processes, is a crucial challenge in addressing environmental concerns [1-2]. According to [3], it is anticipated that by approximately 2050, CO_2 emissions will raise by approximately 70% in comparison to the levels observed in the mid-2010s. Although CO_2 is a major contributor to global warming, nitrogen compounds are also a significant environmental concern due to their negative impact on air quality and public health. NO (nitric oxide) is a toxic gas that is formed at high temperatures during combustion processes, particularly in internal combustion engines. NO can cause respiratory problems, particularly in those with pre-existing respiratory conditions [5, 6].

Internal combustion engines, which power most motor vehicles, are responsible for generating nearly half of the atmosphere's NO_x, CO (carbon monoxide), and hydrocarbon pollutants [7]. According to studies carried out in 2011, vehicles powered by internal combustion engines are responsible for 90% of the air pollution in Sao Paulo, Brazil [8]. Meanwhile, internal combustion engines have contributed during the last 20 years between 4 and 40% of world pollution [9]. Thus, in view of the environmental challenges posed by the use of diesel and gasoline-powered vehicles, public policies are being formulated to phase out the sale and circulation of such vehicles in the near future. France and the United Kingdom announced the end of the sales of cars powered by these engines by 2040. This example is followed

by other European countries, such as Germany, and in emerging countries, such as China and India [10].

Numerous research centers and industries are currently directing their attention towards the development of Carbon Capture and Storage (CCS) technologies. Some of these technologies include pre-combustion capture, post-combustion capture, and oxy-fuel combustion [3, 11]. Oxy-fuel combustion is the process of combusting hydrocarbon fuel in a nearly pure oxygen environment, as opposed to air. Due to the absence of nitrogen in the intake charge, NO_x emissions will be eliminated. As a result, CO_2 and water vapors are the only combustion products [12].

To assume that the exhaust gases resulting from fuel and air combustion are in chemical equilibrium is a useful approximation. This equilibrium scheme serves as the foundation for predicting the quantities of exhaust pollutants, such as NO and CO, in a kinetically controlled manner [13]. The process of combustion in which a fuel is entirely consumed in the presence of stoichiometric air is referred to as theoretical (or stoichiometric) combustion. This theoretical scenario represents an optimal state in which the ideal balance between oxygen and fuel generates the most heat possible, and maximum combustion efficiency is achieved. There are no unburned combustibles and no excess air [14]. In this case, for $C_\alpha H_\beta$ type fuel, N_2, CO_2, and H_2O are the only reaction products. Despite the presence of ample oxygen to completely oxidize all fuel, this approach may not yield precise results due to the dissociation of combustion products that occur at high temperatures [10, 15]. The product composition resulting from fuel-air combustion depends on stoichiometry. For example, if the reactants are fuel-rich, there is not enough oxygen to react completely with the fuel, resulting in the formation of additional products such as CO and H_2, and if the mixture is fuel-lean, there is not enough fuel to consume the oxygen, so there will be unburned oxygen in the product mixture [16]. The equilibrium composition of octane (C_8H_{18})-air mixtures for different temperatures at ϕ = 0.8, 1.0, and 1.2 is presented in [16], with the assumption that the air is composed of 21% oxygen and 79% nitrogen by volume, which means a molar ratio of 1:3.76 between O_2 and N_2. At low temperatures, for the rich case, the major product species present are N_2, H_2O, CO_2, CO and H_2 whereas for the lean case N_2, H_2O, CO_2, and O_2. But at higher temperatures (greater than 2200K), these major species dissociate and react to form additional species in significant amounts [9, 10, 15]. To propose a numerical model that accurately predicts the equilibrium products present in a combustion chamber, a chemical equilibrium scheme that accounts for a specific number of species must be utilized [9, 10]. Thus, in this case study, we consider the equilibrium combustion model with 10 species, applied for equivalence ratio $\emptyset < 3$, as suggested in [16]. The equilibrium compositions are determined by adapting the equilibrium-constant approach routines of [13], as presented in [16], to the specific conditions of oxy-fuel combustion. The aim of the present study is to numerically investigate the effect of altering the oxygen content in the reaction mixture from 21% to 100% on the equilibrium composition of C_8H_{18} combustion.

II. METHODOLOGY

We modify the chemical reaction from the 10 species model [16] to allow changes in the oxygen and nitrogen percentage to simulate oxy-fuel combustion. Let us consider the following reaction:

$$\epsilon\emptyset C_\alpha H_\beta O_\gamma N_\delta + xO_2 + (1-x)N_2 \rightarrow y_1CO_2 + y_2H_2O + y_3N_2 + y_4O_2 + y_5CO + y_6H_2 + y_7H + y_8O + y_9OH + y_{10}NO \quad (1)$$

where x ($0.21 < x < 1.0$) is the oxygen percentage.

The atomic balance yield is described by four equations:

$$\text{C:} \quad \epsilon\emptyset\alpha = (y_1 + y_5)M \quad (2)$$

$$\text{H:} \quad \epsilon\emptyset\beta = (2y_2 + 2y_6 + y_7 + y_9)M \quad (3)$$

$$\text{O:} \quad \epsilon\emptyset\gamma + 2x = (2y_1 + y_2 + 2y_4 + y_5 + y_8 + y_9 + y_{10})M \quad (4)$$

$$\text{N:} \quad \epsilon\emptyset\delta + 2(1-x) = (2y_2 + y_{10})M \quad (5)$$

where M is the total number of moles. The sum of mole fractions results in:

$$\sum_{i=1}^{10} y_i - 1 = 0 \quad (6)$$

This equation introduces the six equilibrium constants that will give 11 equations for the 10 unknown mole fractions (y_i) and the number of moles (M). The reactions are:

$$\frac{1}{2}H_2 \rightleftharpoons H \qquad K_1 = \frac{y_7 P^{1/2}}{y_6^{1/2}} \quad (7)$$

$$\frac{1}{2}O_2 \rightleftharpoons O \qquad K_2 = \frac{y_8 P^{1/2}}{y_4^{1/2}} \quad (8)$$

$$\frac{1}{2}H_2 + \frac{1}{2}O_2 \rightleftharpoons OH \qquad K_3 = \frac{y_9}{y_4^{1/2} y_6^{1/2}} \quad (9)$$

$$\frac{1}{2}O_2 + \frac{1}{2}N_2 \rightleftharpoons NO \qquad K_4 = \frac{y_{10}}{y_4^{1/2} y_3^{1/2}} \quad (10)$$

$$\frac{1}{2}O_2 + H_2 \rightleftharpoons H_2O \qquad K_5 = \frac{y_2}{y_4^{1/2} y_6 P^{1/2}} \quad (11)$$

$$\frac{1}{2}O_2 + CO \rightleftharpoons CO_2 \qquad K_6 = \frac{y_1}{y_5 y_4^{1/2} P^{1/2}} \quad (12)$$

The equilibrium constants $K_i(T)$ are fitted as:

$$\log K_p = A \ln\left(\frac{T}{1000}\right) + \frac{B}{T} + C + DT + ET^2 \quad (13)$$

where T is the temperature, $600 < T < 4000K$ [13].

The equilibrium constant expressions can be rearranged to express the mole fractions of the 10 species, all in terms of y_3, y_4, y_5 and y_6, i.e., molar fractions of N_2, O_2, CO and H_2, respectively.

$$y_7 = c_1 y_6^{1/2},\ c_1 = \frac{K_1}{P^{1/2}} \quad (14)$$

$$y_8 = c_2 y_4^{1/2},\ c_2 = \frac{K_2}{P^{1/2}} \quad (15)$$

$$y_9 = c_3 y_4^{1/2} y_6^{1/2},\ c_3 = K_3 \quad (16)$$

$$y_{10} = c_4 y_4^{1/2} y_3^{1/2},\ c_4 = K_4 \quad (17)$$

$$y_2 = c_5 y_4^{1/2} y_6,\ c_5 = K_5 P^{1/2} \quad (18)$$

$$y_1 = c_6 y_4^{1/2} y_5, c_6 = K_6 P^{1/2} \quad (19)$$

By establishing connections between the derived equations and eliminating shared terms, 4 equations can be derived, each with 4 unknownsy_3, y_4, y_5 and y_6, i.e.:

$$f(y_3, y_4, y_5, y_6) = 0 \quad (20)$$

Equation (20) constitutes a nonlinear equation system that necessitates an iterative solution via a numerical approach. In this study, we employed the Newton-Raphson method, and initialized the iterative process with mole fractions derived from a low-temperature combustion model featuring 6 species. We developed a MATLAB code based on the computational routines of [13], as presented in [16], adapted to the specific conditions of oxy-fuel combustion. A more comprehensive account of the methodology can be found in [16, 17].

III. RESULTS AND DISCUSSIONS

We compared the equilibrium composition of octane (C_8H_{18})-air mixtures for 21% O_2 and 79% N_2 to the reaction products when using the parameters in Table I.

TABLE I. PARAMETERS USED IN NUMERICAL SIMULATIONS

Fuel	% Oxygen	Temperature	Fuel-air equivalence ratio	Pressure
Octane (C_8H_{18})	21, 50, 65, 80, 95 and 99	1500K - 3150K	0.8, 1.0, and 1.2	50 bar

Figures 1-3 illustrate the composition shifts with temperature and equivalence ratio for the combustion of C_8H_{18} considering the parameters presented in Table I. In Figure 1, C_8H_{18}-air mixture (21% oxygen and 79% nitrogen by volume) is assumed and the results are very similar to those found in [13, p. 87]. At low temperatures, for the stoichiometric ($\emptyset = 1$) case, the major products species present are N_2, H_2O, and CO_2 (Table II). For lean ($\emptyset = 0.8$) and rich ($\emptyset = 1.2$) cases, although N_2, H_2O and CO_2 are still the main product species, other species arise. For the lean case, a significant amount of O_2 is present, whereas for the rich case there are CO and H_2. When the temperature of the reaction rises, the predominant species dissociate and react resulting in relevant additional species. Notice that in this case there is an exponential rise in product species such as CO, NO, OH, O_2, O, H_2, and H. For lean conditions, the O_2 fraction remains relatively unaffected by the changes in temperature. For rich conditions, the H_2 fraction initially decreases, but subsequently rises with increasing temperature. The product species CO and H_2 generally increase with equivalence ratio, while the O_2, NO, OH, and O mole fractions decrease. It is important to notice that, at high temperatures, a considerable amount of NO is produced, which is significant even in relatively low concentration because it is an air pollutant. Figures 2-3 clearly show that N_2 mole fraction decreases for all equivalence ratios and temperatures while H_2O and CO_2 rise as the oxygen percentage increases. In general, the whole of the analysis done for the case with 21% O_2 still stands because the curves have analogous behavior. At lower temperatures, significant amounts of oxygen can still be observed in the lean case, while the rich case shows high levels of CO and H_2. As the temperature increases, the levels of other species continue to rise exponentially.

TABLE II. PERCENTAGE OF THE SUM N_2+H_2O+CO_2 FOR $\emptyset$ = 1.0

	% Oxygen					
Temperature	**21**	**50**	**65**	**80**	**95**	**99**
2000 K	99.52	99.23	99.12	99.04	98.97	98.96
3150 K	83.54	69.74	64.12	59.23	55.02	54.07

Table II provides insight into the impact of varying the oxygen input on the sum of products N_2, H_2O, and CO_2 at different temperatures for the stoichiometric case ($\emptyset = 1.0$). It is noteworthy that for a temperature of 2000K, the sum of products is relatively insensitive to changes in oxygen input. However, at a higher temperature of 3150K, although N_2 still tends to zero, there is a significant decrease in the sum of products with increasing oxygen input. Notice that for 99% of oxygen at 2000K the percentage of H_2O and CO_2 are 52.19% and 46.04% (Table III) and at 3150K they are 35.49% and 18.10% (Table IV), respectively. Thus, there is a reduction on CO_2 and H_2O formation with increasing oxygen amount and temperature, which is also observed in air combustion (Figure 1). Overall, the results presented in Tables II-IV underscore the complex interplay of various factors in oxy-combustion, and emphasize the importance of a holistic approach to achieving the desired outcomes in combustion systems.

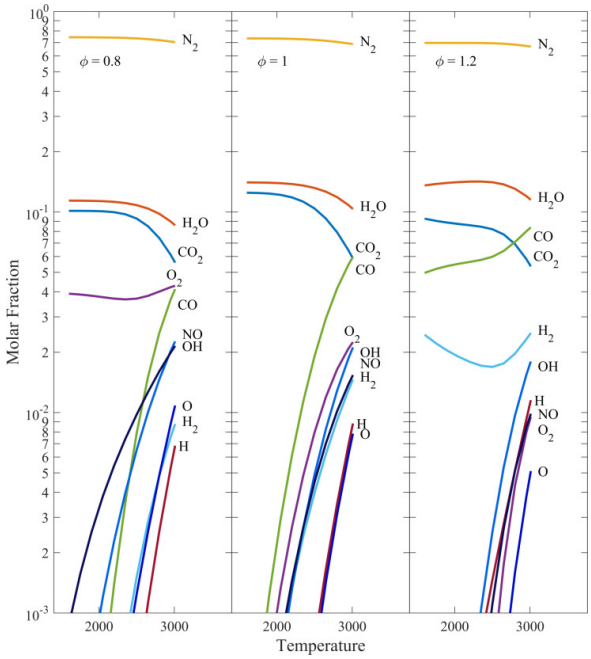

Fig. 1. Equilibrium composition of C_8H_{18}-air mixtures for different temperatures at $\emptyset = 0.8, 1.0$ and 1.2 for $0.21O_2 + 0.79N_2$.

Figure 4 shows the ratio between the molar fraction of product species for 80% O_2 (Figure 3) and 21% O_2 (Figure 1) combustion. The Figure provides a visual representation of the changes for all 10 product species when the oxygen percentage is increased. In this representation, all product species with ratios smaller than 1 decrease with an increase in oxygen

concentration. Conversely, those product species with ratios greater than one exhibit an increase with an increase in oxygen concentration.

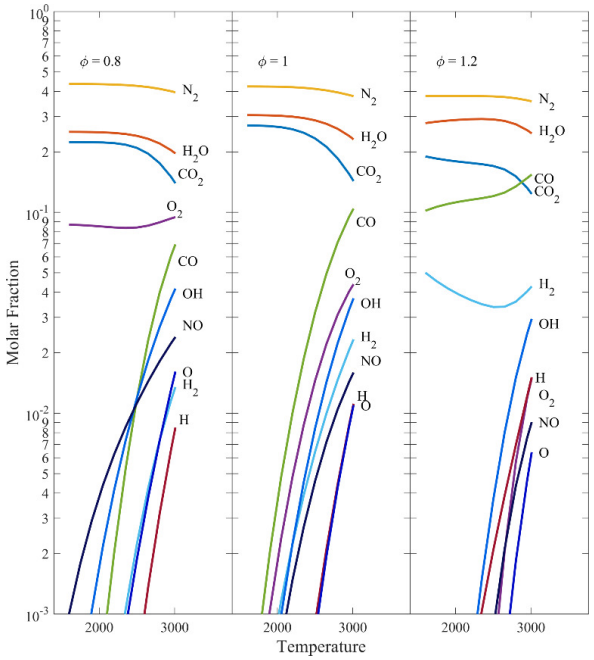

Fig. 2. Equilibrium composition of C_8H_{18} combustion for $0.5O_2$ for different temperatures at $\emptyset = 0.8$, 1.0, and 1.2.

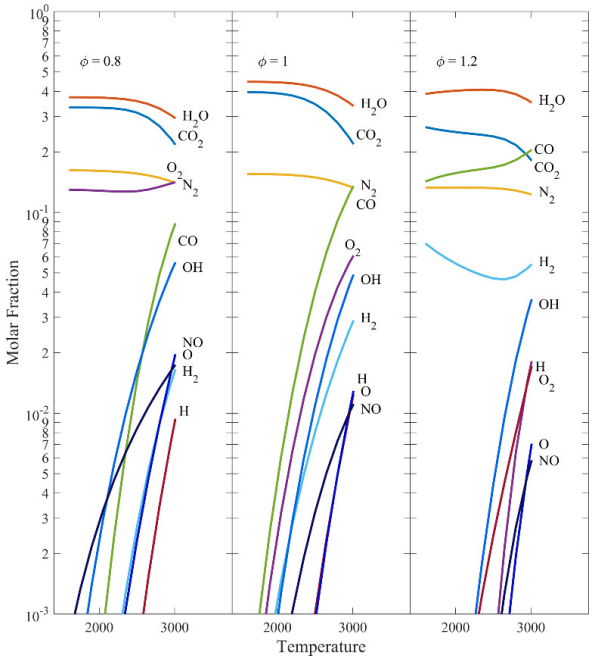

Fig. 3. Equilibrium composition of C_8H_{18} combustion for $0.8O_2$ for different temperatures at $\emptyset = 0.8$, 1.0, and 1.2.

It should be noticed that the molar fraction of N_2 for 80% O_2 combustion has decreased to around 20% compared to the 21% O_2 combustion. In addition, it is observed that N_2 reduction is almost insensitive to temperature. In the case of NO, it is observed that it also reduces but for the lean ($\emptyset$ = 0.8) case, 85% of its content remains. Nevertheless, when $\emptyset$ = 1.2, the concentration of NO remains approximately 45% at low temperatures, but it progressively increases at higher temperatures, reaching nearly 60% at 3000K. The amount of CO_2, H_2O, and O_2 at low temperature and $\emptyset$ =0.8 increased nearly 3.3 times. The amount of CO_2 tends to rise with the temperature for all values of equivalence ratio. CO generally increases with the equivalence ratio and with temperature for $\emptyset$ = 0.8 and $\emptyset$ = 1.0 but tends to decrease for high temperatures and $\emptyset$ = 1.2.

Tables III and IV show the percentages of all products from some variations of the parameters shown in Table I. It is worth noting that for T = 2000K (Table III), the variation of all products is very low between 95-99% oxygen, except for N_2 and NO. Tables V and VI show the reduction rates of N_2 in intervals of input O_2. The reduction of N_2 as a function of O_2 is not constant. From 21%-50% of O_2, for every 1% increase in O_2, there is a reduction of 1.07% of N_2, while between 95%-99% of O_2, for every 1% increase, the reduction of N_2 is 0.74%. Overall, from 21% to 99% of O_2, the rate of reduction of N_2 is 0.93.

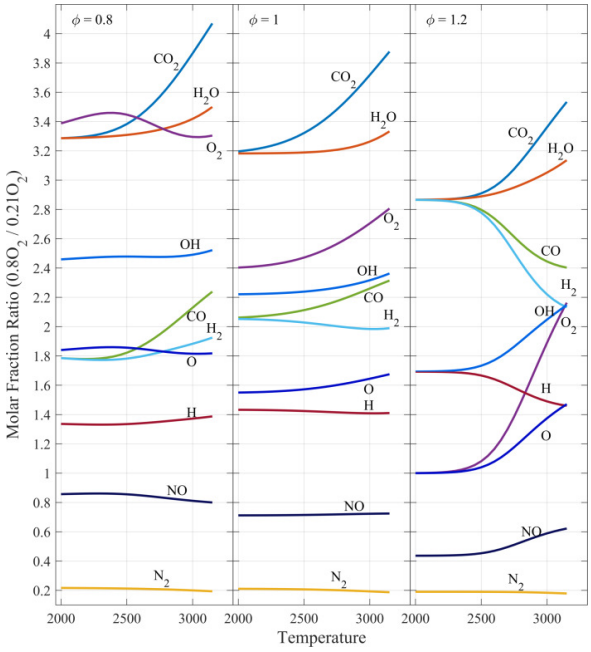

Fig. 4. Ratio ($0.8O_2$ / $0.21O_2$) of the product species for different temperatures at $\emptyset$ = 0.8, 1.0, and 1.2.

TABLE III. VARIATION OF THE % OF EACH PRODUCT VERSUS % OF OXYGEN INPUT FOR T=2000K AND $\emptyset$ = 1

	% Oxygen					
	21	50	65	80	95	99
N_2	73.31	42.24	28.26	15.46	3.70	0.73
H_2O	13.96	30.30	37.67	44.41	50.62	52.19
CO_2	12.25	26.68	33.20	39.16	44.65	46.04
CO	2.25E-01	3.66E-01	4.19E-01	4.63E-01	4.99E-01	5.06E-01
O_2	1.03E-01	1.83E-01	2.16E-01	2.47E-01	2.76E-01	2.85E-01
H_2	5.66E-02	9.19E-02	1.05E-01	1.16E-01	1.25E-01	1.27E-01
NO	5.48E-02	5.56E-02	4.94E-02	3.90E-02	2.02E-02	9.10E-03

OH	4.26E-02	7.25E-02	8.43E-02	9.45E-02	1.04E-01	1.06E-01
H	1.70E-03	2.20E-03	2.40E-03	2.50E-03	2.60E-03	2.60E-03
O	1.00E-03	1.30E-03	1.40E-03	1.50E-03	1.60E-03	1.60E-03

TABLE IV. VARIATION OF THE % OF EACH PRODUCT VERSUS % OF OXYGEN INPUT FOR T=3150K AND $\emptyset = 1$

	% Oxygen					
	21	**50**	**65**	**80**	**95**	**99**
N_2	67.39	36.56	23.79	12.61	2.80	0.48
H_2O	9.08	20.62	25.70	30.27	34.43	35.49
CO_2	7.07	12.56	14.63	16.35	17.79	18.10
CO	4.56	11.47	14.70	17.69	20.50	21.26
O_2	2.73	4.89	5.72	6.44	7.09	7.27
H_2	2.56	5.12	6.19	7.17	8.14	8.46
NO	1.90	1.98	1.76	1.38	0.69	0.29
OH	1.88	3.02	3.42	3.74	4.00	4.04
H	1.51	1.91	2.03	2.13	2.20	2.21
O	1.32	1.87	2.06	2.21	2.36	2.40

TABLE V. DECAY RATE ANALYSIS, T=2000K, $\emptyset = 1$

% oxygen (interval)	21-50	50-65	65-80	80-95	95-99	**21-99**
Decay rate	-1,07	-0.93	-0.85	-0.78	-0.74	**-0.93**

TABLE VI. DECAY RATE ANALYSIS, T=3150K, $\emptyset = 1$

% oxygen (interval)	21-50	50-65	65-80	80-95	95-99	**21-99**
Decay rate	-1,06	-0.85	-0.745	-0.65	-0.58	**-0.858**

IV. CONCLUSIONS

The study of the oxy-combustion of C_8H_{18} presented in this paper provides valuable insights into the equilibrium products that can be formed during the combustion of this fuel using a 10-species model. Significantly, we emphasize that the reduction of N_2 is not uniform and varies with the amount of present O_2. The reduction rate of N_2 was observed to be 0.93 overall, covering the range of O_2 percentages between 21% to 99%. The methodology and approach used in this study can also be applied to analyze the products of other types of hydrocarbon fuels ($C_\alpha H_\beta O_\gamma N_\delta$), which is important for predicting the quantities of exhaust pollutants such as NO and CO in a kinetically controlled fashion. Furthermore, the assumption that the burned gases produced by the combustion of fuel and air are in chemical equilibrium is a good approximation for steady-state operating conditions in internal combustion engines. This simplifies the modeling of the combustion process and enables the use of thermodynamic cycle models to estimate engine performance.

Although significant progress has been made in the study of oxy-combustion during the recent years, it remains a rapidly evolving field with several challenges and open questions that require further investigation. These challenges include issues such as flame instability and the cost of operating an oxy-combustion system. In conclusion, while oxy-combustion offers many potential benefits, there are still significant technical and economic challenges that need to be addressed. Further research and development efforts are needed to overcome these challenges and fully realize the potential of oxy-combustion for clean and efficient energy production.

ACKNOWLEDGMENT

This research was funded by CAPES (Procs. 23038.000263/2022-19) and CNPq (Procs. 426823/2018-4).

REFERENCES

[1] V. H. M. Nguyen, L. D. L. Nguyen, C. V. Vo, and B. T. T. Phan, "Green Scenarios for Power Generation in Vietnam by 2030," *Engineering, Technology & Applied Science Research*, vol. 9, no. 2, pp. 4019–4026, Apr. 2019, https://doi.org/10.48084/etasr.2658.

[2] J. Furlan, J. A. Martins, and E. C. Romão, "Dispersion of toxic gases (CO and CO2) by 2D numerical simulation," *Ain Shams Engineering Journal*, vol. 10, no. 1, pp. 151–159, Mar. 2019, https://doi.org/10.1016/j.asej.2018.03.010.

[3] M. Lupion, R. Diego, L. Loubeau, and B. Navarrete, "CIUDEN CCS Project: Status of the CO2 capture technology development plant in power generation," *Energy Procedia*, vol. 4, pp. 5639–5646, Jan. 2011, https://doi.org/10.1016/j.egypro.2011.02.555.

[4] M. A. Habib and M. A. Nemitallah, "Design of an ion transport membrane reactor for application in fire tube boilers," *Energy*, vol. 81, pp. 787–801, Mar. 2015, https://doi.org/10.1016/j.energy.2015.01.029.

[5] W. R. do Prado Junior, J. A. Martins, and E. C. Romao, "Utilizing Numerical Simulations to Analyze the Efficiency of a Porous Reactor," *Engineering, Technology & Applied Science Research*, vol. 12, no. 3, pp. 8755–8759, Jun. 2022, https://doi.org/10.48084/etasr.4957.

[6] Q. B. Jamali *et al.*, "Analysis of CO2, CO, NO, NO2, and PM Particulates of a Diesel Engine Exhaust," *Engineering, Technology & Applied Science Research*, vol. 9, no. 6, pp. 4912–4916, Dec. 2019, https://doi.org/10.48084/etasr.3093.

[7] S. Turns, *An Introduction to Combustion: Concepts and Applications*, 3rd ed. New York, NY, USA: McGraw Hill, 2011.

[8] A. Braga, L. A. A. Pereira, G. M. Böhm, and P. Saldiva, "Poluição atmosférica e saúde humana," *Revista USP*, no. 51, pp. 58–71, Nov. 2001, https://doi.org/10.11606/issn.2316-9036.v0i51p58-71.

[9] F. Leach, "A negative emission internal combustion engine vehicle?," *Atmospheric Environment*, vol. 294, Feb. 2023, Art. no. 119488, https://doi.org/10.1016/j.atmosenv.2022.119488.

[10] D. Fernandes, "Por que os carros movidos a gasolina e diesel estão com os dias contados em países europeus e vários emergentes," *BBC News Brasil*, Nov. 20, 2017.

[11] G. Scheffknecht, L. Al-Makhadmeh, U. Schnell, and J. Maier, "Oxy-fuel coal combustion—A review of the current state-of-the-art," *International Journal of Greenhouse Gas Control*, vol. 5, pp. S16–S35, Jul. 2011, https://doi.org/10.1016/j.ijggc.2011.05.020.

[12] L. Zheng, Ed., *Oxy-Fuel Combustion for Power Generation and Carbon Dioxide (CO2) Capture*. Woodhead Publishing, 2011.

[13] C. Olikara and G. L. Borman, "A Computer Program for Calculating Properties of Equilibrium Combustion Products with Some Applications to I.C. Engines," SAE International, Warrendale, PA, USA, SAE Technical Paper 750468, Feb. 1975, https://doi.org/10.4271/750468.

[14] D. S. Fox *et al.*, "Natural Gas/Oxygen Burner Rig at The NASA Glenn Materials Research Laboratory," NASA, Cleveland, OH, USA, NASA/TM-20220002202, 2022.

[15] J. Heywood, *Internal Combustion Engine Fundamentals*, 1st ed. New York, NY, USA: McGraw-Hill Education, 1988.

[16] C. R. Ferguson and A. T. Kirkpatrick, *Internal Combustion Engines: Applied Thermosciences*, 3rd ed. Chichester, West Sussex, UK: Wiley, 2015.

[17] H. K. Kayadelen and Y. Ust, "Prediction of equilibrium products and thermodynamic properties in H2O injected combustion for CαHβOγNδ type fuels," *Fuel*, vol. 113, pp. 389–401, Nov. 2013, https://doi.org/10.1016/j.fuel.2013.05.095.